Efficient gene targeting by homology-directed repair in rat zygotes using TALE nucleases

Séverine Remy, Laurent Tesson, Séverine Menoret, et al.

Genome Res. 2014 24: 1371-1383 originally published online July 2, 2014
Access the most recent version at doi:10.1101/gr.171538.113

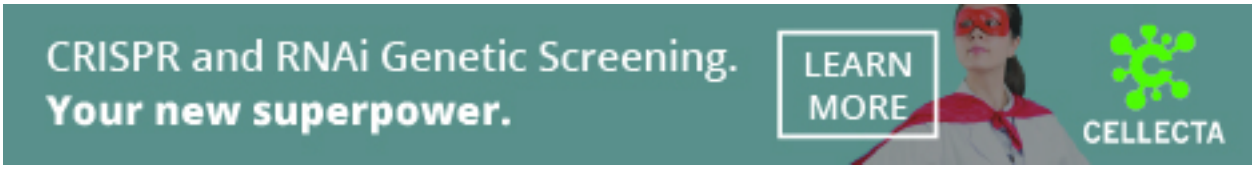

Method

Efficient gene targeting by homology-directed repair in rat zygotes using TALE nucleases

Séverine Remy,[1,2,7] Laurent Tesson,[1,2,7] Séverine Menoret,[1,2] Claire Usal,[1,2] Anne De Cian,[3] Virginie Thepenier,[1,2] Reynald Thinard,[1,2] Daniel Baron,[1] Marine Charpentier,[3] Jean-Baptiste Renaud,[3] Roland Buelow,[4] Gregory J. Cost,[5] Carine Giovannangeli,[3] Alexandre Fraichard,[6] Jean-Paul Concordet,[3] and Ignacio Anegon[1,2]

[1]INSERM UMR 1064-ITUN, CHU de Nantes, Nantes F44093, France; [2]Platform Rat Transgenesis, Nantes F44093, France; [3]INSERM U565, CNRS UMR7196, Museum National d'Histoire Naturelle, F75005 Paris, France; [4]Open Monoclonal Technologies, Palo Alto, California 94303, USA; [5]Sangamo BioSciences, Richmond, California 94804, USA; [6]genOway, Lyon F69007, France

The generation of genetically modified animals is important for both research and commercial purposes. The rat is an important model organism that until recently lacked efficient genetic engineering tools. Sequence-specific nucleases, such as ZFNs, TALE nucleases, and CRISPR/Cas9 have allowed the creation of rat knockout models. Genetic engineering by homology-directed repair (HDR) is utilized to create animals expressing transgenes in a controlled way and to introduce precise genetic modifications. We applied TALE nucleases and donor DNA microinjection into zygotes to generate HDR-modified rats with large new sequences introduced into three different loci with high efficiency (0.62%–5.13% of microinjected zygotes). Two of these loci (*Rosa26* and *Hprt1*) are known to allow robust and reproducible transgene expression and were targeted for integration of a GFP expression cassette driven by the CAG promoter. GFP-expressing embryos and four *Rosa26* GFP rat lines analyzed showed strong and widespread GFP expression in most cells of all analyzed tissues. The third targeted locus was *Ighm*, where we performed successful exon exchange of rat exon 2 for the human one. At all three loci we observed HDR only when using linear and not circular donor DNA. Mild hypothermic (30°C) culture of zygotes after microinjection increased HDR efficiency for some loci. Our study demonstrates that TALE nuclease and donor DNA microinjection into rat zygotes results in efficient and reproducible targeted donor integration by HDR. This allowed creation of genetically modified rats in a work-, cost-, and time-effective manner.

[Supplemental material is available for this article.]

Modifying the genome of animals is crucial for an in-depth understanding of physiological and pathophysiological processes as well as for commercial development. Mouse models have traditionally been used in genetics over the past decades, since researchers have in hand all the tools (in particular, embryonic stem [ES] cells) to perform homology-directed repair (HDR) in order to manipulate precisely the genome of this organism (Capecchi 2005). Unfortunately, until recently, HDR-mediated gene targeting was not possible in most other species, including the rat. The rat is a preferred species for studying physiology and certain human pathologies (Jacob 1999, 2010; Jacob and Kwitek 2002). Thus, precise gene targeting technologies would allow many important biomedical questions to be addressed. Despite the recent derivation of rat ES cells (Buehr et al. 2008; Li et al. 2008) to generate knockout (Tong et al. 2010; Yamamoto et al. 2012) and knock-in rats (Meek et al. 2010), rat ES cells are still less robust than mouse ES cells (Zheng et al. 2012). The emergence of engineered nucleases, allowing the rapid and effective generation of genetically modified animals, opens the door to gene targeting in rat but also in other species for which ES cells are not yet available, and provides a faster and more cost-effective strategy compared to the use of ES cells. We and others have shown that zinc finger nucleases (ZFNs) (Geurts et al. 2009; Mashimo et al. 2010), transcription activator-like effector (TALE) nucleases (Tesson et al. 2011; Tong et al. 2012; Mashimo et al. 2013), meganucleases (Menoret et al. 2013), and the clustered regularly interspaced short palindromic repeats (CRISPR)-associated protein (Cas) system (Li et al. 2013a,b) are highly and reproducibly effective at disrupting endogenous genes in rat zygotes. Mutations introduced are typically small insertions and/or deletions (indels) that result from imprecise repair of nuclease-induced DNA double-strand breaks by the nonhomologous end joining (NHEJ) mechanism. In addition, the presence of donor DNA allows either the insertion of exogenous genetic information or the replacement of an endogenous sequence by the one of interest. Targeting transgene addition or sequence replacement at loci in the mammalian genome by HDR has been demonstrated using ZFNs in mouse (Meyer et al. 2010; Cui et al. 2011; Meyer et al. 2012), rat (Cui et al. 2011), and rabbit (Flisikowska et al. 2011) zygotes. Gene editing in zygotes using TALE nucleases aimed to introduce point mutations (Wang et al. 2013; Wefers et al. 2013; Ponce de Leon et al. 2014) and, only very recently for the first time, an expression cassette in mice (Sommer et al. 2014).

Even if engineered nucleases stimulate HDR events, the frequency of these events remains rare. Finding methods which could increase the cellular activity of these artificial nucleases may en-

[7]These authors contributed equally to this work.
Corresponding author: Ignacio.Anegon@univ-nantes.fr
Article published online before print. Article, supplemental material, and publication date are at http://www.genome.org/cgi/doi/10.1101/gr.171538.113.

hance rates of HDR. It has been reported that accumulation of nuclease proteins induced by a transient hypothermia enhanced the frequency of gene disruption induced both by ZFNs (Doyon et al. 2010) and by TALE nucleases (Miller et al. 2011) in cell lines, suggesting that this strategy could have beneficial effects on the frequency of HDR events in rat zygotes.

In our study, we applied TALE nucleases to achieve the insertion of a large expression cassette or exon exchange through gene targeting by HDR in rat zygotes. For that purpose, we microinjected TALE nuclease pairs designed to target three loci and the corresponding targeting vectors with regions homologous to the nuclease target site. Two targeted loci (*Rosa26* and *Hprt1*) are known to be permissive for transgene expression, and are therefore ideal candidates to integrate a transgene of interest intended to have stable and ubiquitous expression. Indeed, the *Rosa26* locus is commonly used in mice to achieve targeted insertions by HDR using ES cells and has been targeted using ZFNs in mice (Meyer et al. 2010; Hermann et al. 2012). The rat *Rosa26* locus was targeted using ES cells (Kobayashi et al. 2012) but not yet using nucleases. Similarly, the *Hprt* locus is often chosen as a "permissive" locus for targeted integration of transgenes in mouse ES cells (Bronson et al. 1996; Meek et al. 2010). These two loci were chosen to target insertion of a ubiquitous expression cassette encoding GFP, and to assess the potentially beneficial effect of a mild hypothermia treatment on TALE nuclease activity in HDR-mediated transgene integration. The third locus tested was the *Ighm* locus, for which we achieved efficient rat-to-human exon 2 replacement. The results presented demonstrate that TALE nucleases are efficient tools to insert exogenous genetic information or to replace an endogenous sequence with the one of interest.

Results

Activity of *Hprt1.1*, *Hprt1.2*, and *Rosa26* TALE nucleases in cultured rat cells

We designed pairs of TALE nucleases targeting the rat *Hprt1* gene at two different sites (which we refer to as *Hprt1.1* and *Hprt1.2)* within intron 1, or the *Rosa26* locus in intron 1, and examined their cleavage activity in cultured rat C6 cells transfected with plasmid DNA encoding individual TALE nucleases. The cleavage activity of the different TALE nuclease pairs was assessed using the T7 endonuclease assay (Fig. 1). We observed 9%, 15%, and 13% of chromosomes bearing nuclease-induced mutations in rat C6 cells transfected with 2 × 0.75 µg *Hprt1.1*, *Hprt1.2*, or *Rosa26* TALE nuclease pairs, respectively. The frequency of cleavage events increased with higher concentrations (2 × 1.5 µg) of each TALE nuclease pair: 19% for *Hprt1.1*, 21% for *Hprt1.2*, and 17% for *Rosa26*. These results show that all the tested nuclease pairs are active and allowed us to proceed with confidence with experiments in one-cell embryos to achieve targeted knock-in events.

Targeting integration into the rat *Hprt1* and *Rosa26* loci

In order to test whether TALE nucleases could stimulate targeted transgene integration by HDR, we chose to introduce a ubiquitous *GFP* expression cassette (CAG-GFP-BGHpA) of 3142 bp, flanked by 5′ and 3′ homology arms of 800 bp each contiguous to the TALE nuclease cleavage point (Figs. 2A, 3A).

TALE nuclease mRNA and linear donor DNA were co-injected into one-cell stage embryos at different concentrations for the TALE nucleases and at 2 ng/µl for the linear donor DNA (excised expression cassette and homology arms). As previously described (Meyer et al. 2010), a two-step microinjection procedure was performed: The TALE nucleases mRNA and donor DNA mixture were first injected into the male pronucleus and then into the cytoplasm during withdrawal of the injection pipette. We cultured injected embryos at either 37°C for 3 h or 37°C for 1 h, followed by 30°C for 2 h or 30°C for 3 h to assess the effect of the temperature on the rate of NHEJ and HDR events. Following this period of culture, surviving zygotes were then transferred into recipient females and genotyping was performed on E15 fetuses or on newborns (Table 1).

When zygotes were injected with the three ratios of *Hprt1.1* mRNA/DNA tested, we did not observe significant differences on egg viability (73.5%, 78.5%, and 72.6%), while a mild decrease in their embryonic development was observed at the highest concentration (13.3%, 10.7%, and 8.2%). Concerning the *Hprt1.2* TALE nucleases, increasing concentrations did not significantly affect zygote viability (85.8%, 72.1%, and 78.3%) but did impair birth rate at the highest concentration (26.2% at 5 + 5/2, 20.3% at 10 + 10/2, and 0% at 20 + 20/2 ng/µl). Finally, for *Rosa26* TALE nucleases, we observed increased toxicity as assayed by zygote viability at higher concentrations (80.8%, 76.7%, and 52.2%); all nuclease concentrations used resulted in similarly lower embryonic development (9.2%, 8.8%, and 10.6%).

The incubation of embryos at 37°C + 30°C or 30°C after microinjection of *Hprt1.2* or *Rosa26* TALE nuclease mRNA did not significantly affect either embryo viability or newborn frequencies.

To identify GFP-expressing animals either due to random integration (RI) and/or HDR, E15 fetuses and pups were first exposed to UV light to assay for GFP expression (Table 1). The positive animals were then confirmed by PCR using primers specific for *GFP* (data not shown). The strategies used to analyze the donor DNA integration into *Hprt1* and *Rosa26* targeted loci are illustrated in Supplemental Figure S1 and Figures 2A and 3A. The animals harboring HDR events were identified by PCR amplification of the 5′ and 3′ junctions between the donor sequence and the target locus (Figs. 2B, 3B; Supplemental Fig. S1B; data not shown). The integrity of the 5′ and 3′ junctions was confirmed by sequencing (Figs. 2D, 3C; data not shown).

No GFP-expressing animals or animals with donor DNA integration were observed when high concentrations (20 + 20 or 50 + 50 ng/µl) of mRNA encoding *Hprt1.1*, *Hprt1.2*, or *Rosa26* TALE nucleases were injected, probably at least in part due to toxicity (Table 1). With *Hprt1.1*, *Hprt1.2*, or *Rosa26* TALE nucleases at a ratio of 10 + 10/2 ng/µl mRNA/DNA (37°C condition), the frequency of DNA integration reached 1.02%, 0.63%, and 3.30% of transferred embryos, respectively (Table 1). In these conditions, junction PCR analyses revealed that one *Hprt1.1* (13.1) (Table 2), one *Hprt1.2* (6.1) (Table 2), and two *Rosa26* (2.1 and 3.1) (Fig. 3B) founders harbored an HDR profile, whereas one *Rosa26* was a RI (5.3) (Table 2). Lower concentrations (5 + 5/2 ng/µl) of *Hprt1.2* and *Rosa26* TALE nucleases were also very efficient at inducing donor DNA integration (3.17% and 1.67% of transferred embryos GFP+, respectively) by HDR (three out of four founders for the *Hprt1.2* locus, e.g., 9.6, 11.9, and 12.2, and two founders for the *Rosa26* locus, e.g., 10.2 and 12.5) (Tables 1, 2).

Interestingly, using *Hprt1.2* TALE nucleases, the HDR frequency of embryos cultured at 37°C for 3 h (0.63 and 2.38% at the dose of 10 + 10/2 and 5 + 5/2, respectively) was increased when embryos were maintained either at 37°C for 1 h + 30°C for 2 h (2.73 and 2.7 at the dose of 10 + 10/2 and 5 + 5/2, respectively) or 30°C for 3 h (2.54 and 5.13 at the dose of 10 + 10/2 and 5 + 5/2, re-

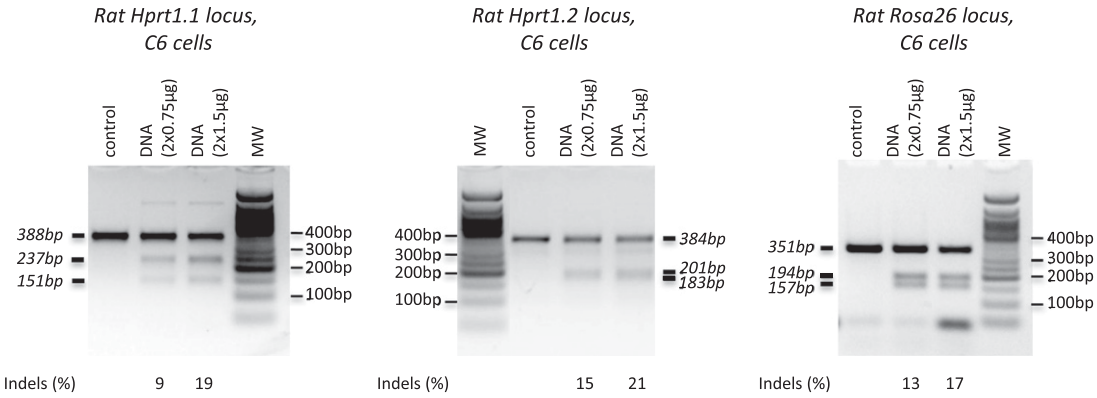

Figure 1. Assay of TALE nucleases for rat *Hprt1.1*, *Hprt1.2*, and *Rosa26* loci. The frequency of TALE nuclease cleavage was determined using T7 endonuclease assay in C6 cells transfected with the indicated amount of rat *Hprt1.1*, *Hprt1.2*, or *Rosa26* TALE nuclease expression vectors. Expression vectors without nucleases serve as negative controls. The expected sizes of undigested and digested fragments are indicated in italics. The efficiency of cleavage is indicated *below* each gel.

spectively) (Table 1). Transient incubation at a lower temperature also tended to increase the frequency of HDR events in the *Rosa26* locus: 2.78 at 37°C for 1 h + 30°C for 2 h vs. 1.67% at 37°C but 0% for 30°C incubation (Table 1). The analyses of indel events due to NHEJ at *Hprt1.2* and *Rosa26* loci showed that their frequency did not vary significantly among the three temperature conditions (Table 1).

RI of the GFP expression cassette (scored as GFP expression and positive PCRs for *GFP* but with negative 5′ and 3′ junction PCRs) occurred at frequencies similar to those observed when linearized DNA is microinjected for the generation of transgenic rats (0.67%–2.54%) (Tesson et al. 2005) and without differences among the different experimental conditions. These RI transgenic animals did not contain HDR events, and for *Hprt1.2* TALE nucleases included animals 13.2, 3.2, 5.7, 6.4, 6.5, 7.5, 7.8, 5.1, 9.5, and 10.8 as well as for *Rosa26*, animals 5.3, 7.1, and 19.3 (Table 2).

To confirm targeted integration of donor DNA by HDR further, we performed Southern blot analyses. All of the 20 animals with the *GFP* transgene integrated into the *Hprt1.2* locus as identified using junction PCR analyses (Figs. 2B,D; Table 2; data not shown), harbored a band of 7.6 kb, consistent with the expected integration mediated by HDR (Fig. 2C; data not shown). The profile on the Southern analysis of some of the animals (animals 2.2 and 5.9 in Fig. 2C) showed a single copy of the expression cassette, whereas that of others (animals 1.2 and 3.4 in Fig. 2C) showed the presence of a band of 4.7 kb compatible with the presence of more than one copy in concatemers. None of these embryos showed additional bands, indicating that they did not harbor RI copies of the expression cassette. PCR analyses were performed to determine the configuration of these concatemers. For the embryos injected with *Hprt1.2* TALE nucleases, all the RI and some of the HDR animals bore integrated concatemers (Table 2) in a head-to-tail configuration (Supplemental Fig. S2B) but not in head-to-head or tail-to-tail (data not shown).

At the *Rosa26* locus, the seven animals for which amplified fragments of expected size and sequence were observed both in 5′ and 3′ junction PCR analyses (Figs. 3B,C; Table 2; data not shown) showed bands of the expected size (9.2 kb and 2.2 kb), consistent with integration at the target locus by HDR (data not shown). Three of these rats had integration of donor concatemers (Supplemental Fig. S2B) in a head-to-tail configuration but not in head-to-head or tail-to-tail (data not shown).

TALE nuclease-induced DNA cleavage was required for efficient targeted donor DNA integration since the microinjection of 2 ng/µl linear donor DNA alone did not result in any HDR positive animals (Table 1), in accordance with a previous publication that showed a very low level of efficacy (<0.1%) for spontaneous HDR in mouse zygotes (Brinster et al. 1989).

We compared the excised linear form of donor DNA vs. the supercoiled form of the plasmid for transgene integration by HDR. As reported in Table 1, of the 25 embryos issued from microinjection of *Hprt1.2* TALE nucleases and circular donor DNA, none integrated donor DNA by HDR, and one of them (circ-4.1) (Table 2) integrated the donor DNA by RI. In comparison, in the same conditions (5 + 5/2 and 30°C incubation), when donor DNA was injected in a linear form we obtained eight GFP+ animals (six by HDR, e.g., 1.2, 2.2, 5.9, 9.7, 10.2, and 10.4, and two by RI, e.g., 6.4 and 6.5) (Tables 1, 2).

In conclusion, targeted transgene integration could be efficiently achieved in all *Hprt1.1*, *Hprt1.2*, and *Rosa26* TALE nuclease injections when the concentration of the TALE nuclease was below 10 ng/µl. The frequency of mutated animals with indel mutations was higher than that of targeted integration by HDR, consistent with NHEJ being the prevalent mechanism for DNA double-strand break repair. In all founders harboring an HDR-mediated transgene insertion except one (*Hprt1.2* 1.1) (Table 2), we found a conserved integrated donor DNA and intact 5′ and 3′ junctions. Transient diminution of temperature and excised linear vs. circular donor DNA tended to increase the frequency of HDR and thus represent alternative methods for gene targeting HDR in rat zygotes that might be superior for certain loci and nuclease pairs.

Efficient germline transmission and expression of donor sequences targeted into the *Rosa26* locus

Five different *Rosa26* founders with HDR of the CAG-*GFP* expression cassette showed germline transmission of the donor sequence with frequencies between 14% and 46% (Supplemental Table S1). Figure 3D illustrates two 8-d-old GFP+ animals in the offspring of the animal *Rosa26* KI 8.4. Moreover, offspring of each of four *Rosa26* HDR+ founders analyzed presented a similar percentage and mean fluorescence intensity of CD45+ GFP+ cells (Fig. 3E). This expression was comparable in animals with one copy (8.4F1, 9.1F1, and 10.2 F1) or with concatemers (12.5F1) (Fig. 3E). Finally,

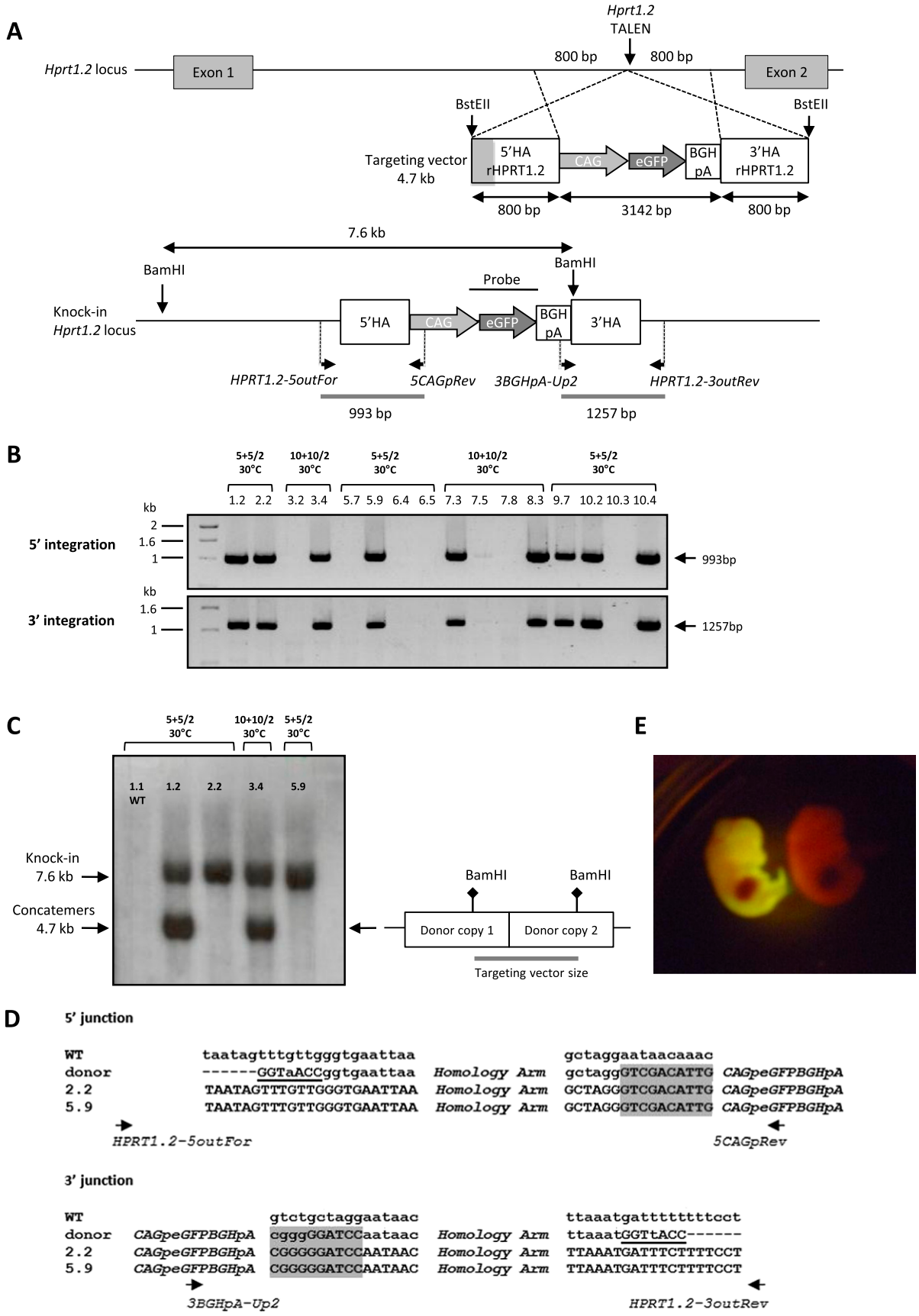

Figure 2. (Legend on next page)

expression of GFP was uniformly detected in most cells of all tissues analyzed, as shown for liver, kidney, and pancreas (Fig. 3D; data not shown). Expression of GFP in embryos generated with *Hprt1.1* and *Hprt1.2* TALE nucleases also showed strong and uniform expression upon in toto analysis (Fig. 2E; data not shown). These data provide evidence that integration of the transgene into the *Rosa26* locus took place early in development, with low mosaicism and high frequency of transmission to the offspring. Additionally, the integrated transgene into the targeted *Rosa26* locus showed high and uniform expression in different lines of transgenic rats, indicating that integration of transgenes into this locus using TALE nucleases is a robust strategy to express transgenes.

Targeted replacement of a rat exon with a human exon at the *Ighm* locus

We aimed to replace an endogenous sequence with an exogenous one since this would allow a wide range of genetic editing applications. As a proof-of-concept model, we applied TALE nucleases targeting the rat *Ighm* locus used in a previous work (Tesson et al. 2011) to obtain an exon exchange directly in rat zygotes. In the previous study, we showed the cleavage activity of this TALE nuclease pair to be 13% in rat S16 cells in vitro and 58% in injected rat zygotes, when delivered as mRNA.

We microinjected sequentially into the pronuclei and cytoplasm of rat zygotes TALE nuclease mRNA directed to sequences in exon 2 of the rat *Ighm* locus, together with donor DNA sequences containing the exon 2 of human *IGHM* (71% homology vs. rat) and homology arms (0.75 and 1.46 kb for 5′ and 3′ arms, respectively) of rat genomic sequence (Fig. 4A). The homology arms were separated from the TALE nucleases cleavage site by ~150 bp. With this transgene donor, successful exon replacement requires spontaneous cellular trimming of at least one of the 3′ single-stranded ends so that the 3′ end terminates in a region of homology with the donor. The microinjection statistics are summarized in Table 3. Microinjection with the supercoiled donor plasmid (410 zygotes) or linearized donor sequences (1063 zygotes) resulted in both cases in normal embryo survival (75.1% and 72.7% of microinjected embryos) and normal numbers of newborn animals (22.9% and 15.8% of transferred embryos). Microinjection of TALE nucleases plus the supercoiled plasmid donor DNA did not result in any donor integration by HDR, but two transgenic animals carrying RI could be detected (Tables 3, 4). Microinjection of TALE nucleases plus the linear donor DNA resulted in eight animals (Table 3) with RI of linear donor DNA (8, 44, 49, 55, 56, 63, 68, and 69) (Table 4) and in one embryo (E3) and two founders (53 and 54) with bona fide targeted integration by HDR (0.62% of the transferred zygotes) since they showed 5′ and 3′ flanking PCRs of the expected size and with intact sequences (Figs. 4B,C) as well as the expected 3.2-kb band on the Southern blot (Fig. 4D). Southern blot analysis showed the presence of donor concatemers at the integration site in one founder (53), whereas the other founder (54) had one copy (Fig. 4D) and embryo E3 showed concatemers (data not shown). PCR analysis of concatemers showed that they were orientated in a head-to-tail orientation (Supplemental Fig. S2D).

Founder 54 was mated and transmitted the transgene to six out of 17 pups (Supplemental Table S1). mRNA products containing rat and human sequences were detected in the offspring by RT-PCRs of the expected size (Fig. 4E; data not shown) and contained intact rat and human sequences (data not shown). These F1 heterozygous animals were mated to obtain homozygous F2 animals which did not show the presence of wild-type rat CH2 sequences, having both alleles replaced with human sequences (data not shown).

Thus, injection of TALE nucleases mRNAs and linear donor DNA with human sequences resulted in the replacement of rat by human *IGHM* sequences by HDR.

Discussion

ZFNs were used to obtain transgene targeted integration in previous studies in mice (Meyer et al. 2010, 2012; Cui et al. 2011), rats (Cui et al. 2011), and rabbits (Flisikowska et al. 2011). Compared to ZFNs, TALE nucleases can be designed with somewhat fewer positional constraints (Miller et al. 2011), allowing targeting of virtually any sequences, with high activities and very low off-target effects (for review, see Segal and Meckler 2013). TALE nucleases were applied to achieve targeted gene addition of point mutations in rodents (Panda et al. 2013; Wang et al. 2013; Wefers et al. 2013; Ponce de Leon et al. 2014) and (after the submission of this manuscript) in mice using an expression cassette (Sommer et al. 2014).

Here, we used newly generated TALE nucleases for the *Hprt1* and *Rosa26* loci and the previously described TALE nucleases for *Ighm* (Tesson et al. 2011). For the *Hprt1* and *Rosa26* TALE nucleases, we observed that the correlations between in vitro and in vivo efficiency activities are such that *Hprt1.2* > *Rosa26* > *Hprt1.1*. Direct comparison of in vitro efficiencies between *Hprt1* and *Rosa26* TALE

Figure 2. Targeted integration of a *GFP* cassette into the *Hprt1.2* locus. (*A*) (*Upper*) Diagram showing schematic representation of the rat *Hprt1.2* locus, with the site of TALE nuclease action (vertical arrows), and of the targeting vector with the expression cassette CAG-eGFP-BGHpA (3142 bp) and the 5′ and 3′ homology arms (800 bp each). The homology arms are contiguous to the TALE nucleases' cleavage point. (Gray) The sequence overlap (433 bp) between 3′ HArHPRT1.1 (cf. Supplemental Fig. S1) and 5′ HArHPRT1.2. BstEII restriction sites are indicated. (*A*) (*Lower*) Diagram showing schematic representation of the *GFP* cassette integration. For flanking PCR analysis, genomic DNA was PCR-amplified with primers situated for the 5′ side: upstream of the 5′ HA arm (HPRT1.2-5outFor) and in the CAG promoter (5CAGpRev); and for the 3′ side: in the BGHpA (3BGHpA-Up2) and downstream from the 3′ HA arm (HPRT1.2-3out Rev). The position of each primer and the corresponding expected size of PCR products are indicated on the schematic knock-in *Hprt1.2* locus. For Southern blot analysis, genomic DNA was digested with BamHI and was probed with a *GFP* probe. A unique band at 7.6 kb is predicted for a correct HDR into the *Hprt1.2* locus. (*B*) Flanking PCR analysis. Gels show the results of analyzing the 5′ and the 3′ extremities of GFP integration into the *Hprt1.2* locus. A representative panel of 16 animals is illustrated, showing the expected bands of 993 bp using the 5′ pair of primers (HPRT1.2-5outFor + 5CAGpRev) and of 1257 bp using the 3′ pair of primers (3BGHpA-Up2 + HPRT1.2-3outRev). The microinjection conditions in terms of mRNA and DNA concentrations, as well as embryo incubation temperatures, are *above* each animal. (*C*) Southern blot analysis following BamH1 DNA digestion for the analysis of transgene site-specific integration into the *Hprt1.2* locus using a *GFP* probe. Four *Hprt1.2*-GFP+ rats with positive junction PCRs showing a unique band at 7.6 kb for a HDR with a single copy of the transgene, or 7.6 kb and 4.7 kb (the size of the transgene) bands when HDR involved transgene concatemers. The diagram at the *right* explains the expected size of the concatemers once linearized. The absence of additional bands demonstrates that there are no RI integration events in these animals. As a negative control, an offspring rat with no *GFP* expression and negative for *GFP* PCR (1.1) showed no bands. (*D*) Sequence comparison at the 5′ and 3′ junctions, with wild-type genomic DNA and donor DNA sequences, of two representative embryos (2.2 and 5.9). In donor DNA, the presence of the BstEII site is indicated in 5′ and 3′ (underlined). The 5′ and 3′ ends of the expression cassette are colored in gray. (*E*) Representative E15 *Hprt1.2* HDR-GFP embryos using a Dark Reader Spot Lamp.

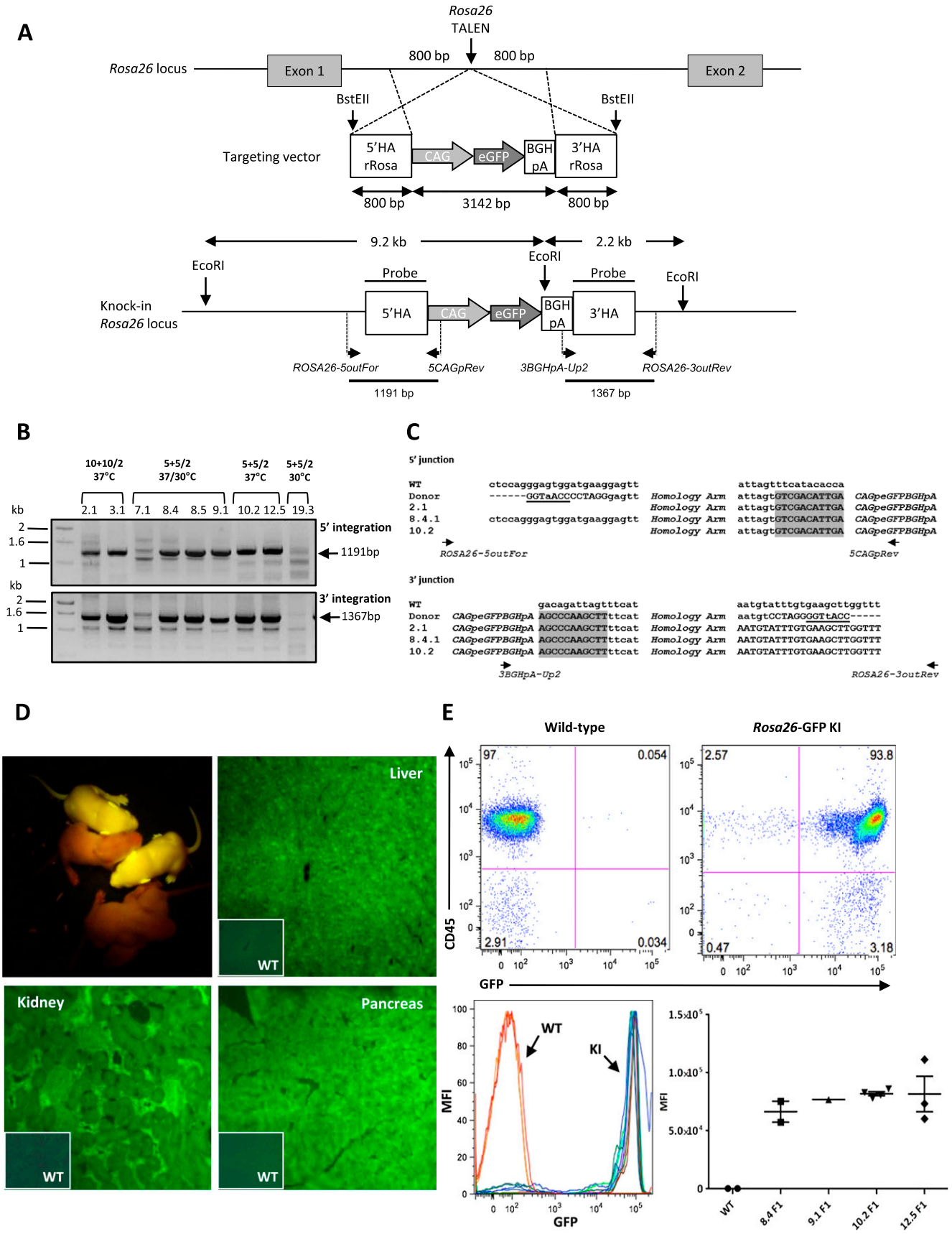

Figure 3. (Legend on next page)

nucleases with those of *Ighm* is difficult since they were transfected in different cell lines.

The efficiency of TALE nuclease-mediated HDR seemed to depend primarily on the efficiency of DNA cleavage by the nuclease and not on the type of locus targeted in terms of expression and chromatin status, since *Hprt1* and *Rosa26* are expressed in the injected zygote, whereas *Ighm* is not. This conclusion is also substantiated by experiments that we performed using a ZFN for the *Ighm* locus with lower nuclease activity (2% in C6 cells and 1.5% of NHEJ following mRNA microinjection) for the exchange of rat by human exon 2 in the *Ighm* locus (same donor DNA as used for the TALE nucleases) that did not result in HDR events (data not shown).

The frequencies of HDR obtained in the present study were between 0.62% and 5.13% of microinjected embryos for the best conditions. Despite differences in the models that make direct comparisons only relative, these frequencies are comparable to the ones for targeted insertion using TALE nucleases and ssODN donors ranging from 1.8% to 6.8% in mouse embryos (Panda et al. 2013; Wefers et al. 2013) but higher than the ones obtained with an expression cassette (2/900, 0.22%) (Sommer et al. 2014). The frequencies obtained in our study are also comparable to the ones observed using ZFN mRNA for HDR in rats (2.4% and 8.3% for two different loci) (Cui et al. 2011) and mice (1.7% and 5% for two different loci) (Meyer et al. 2010; Cui et al. 2011). In this report, as well as in others using ZFNs, TALE nucleases, or CRISPR/Cas (Meyer et al. 2010; Wefers et al. 2013; Auer et al. 2014; Sommer et al. 2014), the NHEJ repair mechanisms occurred always and for each condition at a higher rate than HDR.

A transient cold shock applied to cells lines enhances the cleavage activity of ZFNs (Doyon et al. 2010) and TALE nucleases (Miller et al. 2011), due, at least in part, to an increase in accumulation of nuclease proteins (Doyon et al. 2010), but the effect on HDR was not analyzed. The assessment of this parameter allowed us to show a positive effect of a short or longer incubation at 30°C of injected embryos on the frequency of HDR events but not in the rate of NHEJ, suggesting a preferential repair by the former mechanism. This effect was more accentuated for the *Hprt1.2* locus than for *Rosa26*. Moreover, no or slight effects were observed on viability and embryonic development of rat embryos. Although promising, additional experiments at other loci and in other species are necessary to confirm the generality of these observations.

In HDR strategies using ZFNs or TALE nucleases, donor DNA sequences can be linearized or supercoiled plasmids. In our four HDR insertions (*Hprt1.1, Hprt1.2*, *Rosa26*, and *Ighm*), HDR events were observed when donor DNA was delivered under a linear form, and when directly compared in the *Hprt1.2* and *Ighm* loci, the circular form did not generate HDR events. In other studies using linear or circular DNA donors, the outcomes have been very variable. In the only previous study of HDR in rats using nucleases (ZFNs), both circular and linear forms generated HDR events (Cui et al. 2011; Brown et al. 2013). Using ZFNs in mice, two publications showed that both linear and circular DNA generated HDR (Meyer et al. 2010; Meyer et al. 2012), whereas another publication showed that only the linear, but not the circular form, could result in HDR (Hermann et al. 2012). In *Drosophila*, ZFNs or TALE nucleases induced HDR only using supercoiled plasmid donors (Beumer et al. 2008; Katsuyama et al. 2013). In rabbits, the linear form allowed obtention of HDR when using ZFNs (Flisikowska et al. 2011).

Compared to circular DNA, linear DNA has the potential disadvantage of being more prone to RI into the genome (Brinster et al. 1985). Our results show RI of linearized donor DNA (both the *GFP* expression cassette or human *IGHM* sequences) with frequencies of 0.62% to 1.71% of transferred embryos, close to the frequencies observed when linear DNA is microinjected to generate transgenic rats (Tesson et al. 2005). RI of circular donor DNA was also observed with frequencies of 0.95% and 0.72% for embryos transferred after *Hprt1.2* or *Ighm* TALE nuclease injection, respectively. Therefore, in terms of transgene RI, there is not a significant disadvantage to the use of linear vs. circular donor DNA. Undesirable RI events could be separated from the desired modified allele by breeding (if unlinked to the target locus).

We observed that several of the *Hprt1.1*, *Hprt1.2*, *Rosa26*, and *Ighm* HDR-positive embryos or animals had concatemers. While few studies have analyzed the mechanisms of transgene concatemer formation, one recent one identified NHEJ as the main mechanism of concatamer formation (Dai et al. 2010). It is unclear why concatemers were observed at higher frequencies in the *Hprt1* locus versus the *Rosa26* or *Ighm* loci. Although transgenic animals with RI in concatemers are subject to gene silencing (Garrick et al. 1998), expression of GFP was equivalent in our rats harboring a profile with and without concatemers in the *Rosa26* locus. This similar expression might be due to the insertion in a permissive locus versus RI in sites more prone to methylation. At the same

Figure 3. Targeted integration of a *GFP* cassette into the *Rosa26* locus. (*A*) (*Upper*) Diagram showing schematic representation of the rat *Rosa26* locus, with the site of TALE nuclease action (vertical arrows) and of the targeting vector with the expression cassette (3142 bp) and the 5′ and 3′ homology arms (800 bp each). The homology arms are contiguous to the TALE nucleases' cleavage point. BstEII restriction sites are indicated. (*A*) (*Lower*) Diagram showing schematic representation of the *GFP* cassette integration. For PCR in/out analysis, genomic DNAs were PCR-amplified with primers situated for the 5′ side: upstream of the 5′ HA arm (ROSA26-5outFor) and in the CAG promoter (5CAGpRev); and for the 3′ side: in the BGHpA (3BGHpA-Up2) and downstream from the 3′ HA arm (ROSA26-3out Rev). The position of each primer and the corresponding expected size of PCR products are indicated on the schematic knock-in *Rosa26* locus. For Southern blot analysis, genomic DNA was digested with EcoRI and was probed with the homology arms' probe for *Rosa26*. Two bands at 9.2 kb and 2.2 kb are predicted for a correct HDR into the *Rosa26* locus. (*B*) Flanking PCR analysis. Gels show the results analyzing the 5′ and the 3′ extremities of the expression cassette integration into the *Rosa26* locus. A representative panel of nine founders is illustrated, showing expected bands of 1191 bp using the first pair of primers (ROSA26-5outFor + 5CAGpRev), and of 1367 bp using the second pair of primers (3BGHpA-Up2 + ROSA26-3outRev). The microinjection conditions in terms of mRNA and DNA concentrations as well as embryo incubation temperatures are *above* each animal. (*C*) Sequence comparison at the 5′ and 3′ junctions with wild-type genomic DNA and donor DNA sequences of two representative founders (2.1 and 10.2) and one representative F1 (8.4.1: offspring of founder 8.4). In donor DNA, the presence of the BstEII site is indicated (underlined). The start and the end of the expression cassette are colored in gray. (*D*) Two representative 8-d-old *Rosa26* HDR rat pups (F1s of founder 8.4) and two wild-type littermates. GFP expression in adult tissues (liver, kidney, pancreas) of a *Rosa26* HDR rat. *Insets* show tissues obtained from littermates negative for GFP PCR (wild type, WT). Magnification: ×100. (*E*) GFP expression in leukocytes from different lines of *Rosa26* HDR rats. FACS analysis of GFP expression in CD45+ leukocytes isolated from peripheral blood from four different lines of *Rosa26* HDR adult rats (F1generation) and a wild-type littermate. (*Upper*) FACS patterns obtained from two F1 (an HDR GFP+ and a negative littermate) of founder 8.4. (*Lower*) Analysis of the level of GFP expression in the peripheral blood of offspring of four *Rosa26* HDR founders using the mean fluorescence intensity of leukocytes. Each point represents one animal and the horizontal bars the mean and standard deviations.

Table 1. Microinjection statistics for the *Hprt1.1, Hprt 1.2,* and *Rosa26* loci

Target locus	Dose mRNA/DNA (ng/μl)	Temperature	No. injected eggs (% viable eggs)	No. E15 (e) or pups (p) (%)[a]	No. of GFP+ animals (%)[a]	No. of RI-positive animals (%)[a]	No. of HDR-positive animals (%)[a]	No. of indel-positive animals (%)[a]
Hprt1.1	50 + 50/2	37°C	113 (73.5)	8e (13.3)	0 (0)	0 (0)	0 (0)	1 (1.67)
	20 + 20/2	37°C	209 (78.5)	17e (10.7)	0 (0)	0 (0)	0 (0)	2 (1.26)
	10 + 10/2	37°C	164 (72.6)	8e (8.2)	1 (1.02)	0 (0)	1 (1.02)	2 (2.04)
Hprt1.2	20 + 20/2	37°C	69 (78.3)	0 (0)	0 (0)	0 (0)	0 (0)	0 (0)
	10 + 10/2	37°C	258 (72.1)	32e (20.3)	1 (0.63)	0 (0)	1 (0.63)	15 (9.49)
	10 + 10/2	37°C/30°C	151 (72.8)	19e (17.3)	4 (3.64)	1 (0.91)	3 (2.73)	10 (9.09)
	10 + 10/2	30°C	163 (82.8)	22e (18.6)	6 (5.08)	3 (2.54)	3 (2.54)	6 (5.08)
	5 + 5/2	37°C	148 (85.8)	33e (26.2)	4 (3.17)	1 (0.79)	3 (2.38)	17 (13.5)
	5 + 5/2	37°C/30°C	158 (93.7)	42e (28.4)	6 (4.05)	2 (1.35)	4 (2.70)	24 (16.2)
	5 + 5/2	30°C	173 (79.2)	35e (29.9)	8 (6.84)	2 (1.71)	6 (5.13)	14 (12)
	5 + 5/2 [b]	30°C	159 (71.1)	25e (23.8)	1 (0.95)	1 (0.95)	0 (0)	4 (3.81)
	0/2	30°C	110 (80)	38e (43.2)	0 (0)	0 (0)	0 (0)	na
Rosa26	20 + 20/2	37°C	134 (52.2)	5e (10.6)	0 (0)	0 (0)	0 (0)	1 (2.13)
	10 + 10/2	37°C	180 (76.7)	8e (8.8)	3 (3.30)	1 (1.10)	2 (2.20)	3 (3.30)
	5 + 5/2	37°C	161 (80.8)	11p (9.2)	2 (1.67)	0 (0)	2 (1.67)	5 (4.17)
	5 + 5/2	37°C/30°C	158 (68.4)	21p (19.4)	4 (3.70)	1 (0.92)	3 (2.78)	8 (7.41)
	5 + 5/2	30°C	197 (75.6)	47p (31.5)	1 (0.67)	1 (0.67)	0 (0)	6 (4.03)

Rat *Hprt1.1*, *Hprt1.2*, or *Rosa26* TALE nucleases, as mRNA, were injected at different concentrations each in combination with 2 ng/μl of donor DNA, both into the cytoplasm and into the male pronucleus. Donor DNA was injected either in a linear form with each of the three TALE nuclease pairs or in a circular form only with rat *Hprt1.2* TALE nucleases (see footnote b, below). Injected eggs were maintained under 5% CO_2 at 37°C for 3 h, 37°C for 1 h, followed by 30°C for 2 h, or 30°C for 3 h until reimplantation. Viability was evaluated after the culture period. Potential toxicity was also assessed by the number of day 15 embryos (E15) or of live pups obtained following the transfer of injected eggs. Percentage of the total transferred is indicated in parentheses. The numbers of E15 or live pups which have integrated the donor DNA sequence either by random integration (RI) or HDR integration (PCR positive both at the 5′ and 3′ ends) or which have indel mutations (T7 nuclease assay and sequencing) with no HDR are reported in the last four columns. (na) Not applicable.
[a]Percentages indicated in parentheses correspond to the percentage of transferred embryos.
[b]Donor DNA was injected in a circular form in this condition.

time, expression levels in animals with concatemers were not higher compared to ones with one copy of the transgene, indicating that either some degree of gene silencing has occurred or that some of these extra copies were not intact. In order to improve the efficiency of single-copy transgene integration, concatemer formation may potentially be limited by in situ excision of donor sequences from plasmids. This could be achieved by flanking donor sequences on the injected plasmid by nuclease target sites. Such an approach has been tested in sea urchin and was found to favor HDR in sea urchin embryos injected with ZFNs (Ochiai et al. 2012). The use of a circular donor DNA with a nuclease site for in situ linearization but without any homology arms has also been shown recently to result in high-efficiency homology-independent knock-in of in vitro-transfected cells (Cristea et al. 2013; Maresca et al. 2013) and very recently in zebrafish (albeit concatemers were also observed using this strategy) (Auer et al. 2014). Future studies should compare the efficiency of targeted knock-in by HDR or NHEJ using this in vivo linearized donor DNA approach.

A parameter that can influence HDR following DNA cleavage by nucleases is the distance between the homology arms and the DNA break point. It has been found that the efficiency of gene conversion tracts after double-strand break repair by HDR in cells in vitro rapidly decreases with distance (100 bp) from the nuclease cleavage point (for review, see Johnson and Jasin 2001). In mice microinjected with TALE nucleases, oligonucleotide exchange preferentially occurred in proximity to the double-strand break (Wefers et al. 2013). This is an important point since it may be an obstacle to the exchange of endogenous sequences by new ones. Our results show that the efficiency of HDR using homology arms contiguous to the DNA break, such as in *Hprt1.1, Hprt1.2*, and *Rosa26* loci (1.02%, 0.63%, and 2.2%, respectively), were roughly comparable to that for the *Ighm* locus (0.62%) with homology at ~150 bp from the DNA break point.

Transgenes expression can be influenced by the local environment (position effects) that can lead to transgene silencing or aberrant expression (Milot et al. 1996; Pedram et al. 2006; Gao et al. 2007; Williams et al. 2008). In contrast, targeted integration of DNA sequences into permissive loci, such as *Hprt/Hprt1* (Bronson et al. 1996; Meek et al. 2010) or *Rosa26* (Zambrowicz et al. 1997), by HDR in ES cells is usually chosen for expressing exogenous transgenes. Different ubiquitous promoters have been compared for levels of expression once inserted in the *Rosa26* locus, and CAG was the strongest (Chen et al. 2011). Targeted insertion using nucleases has only been reported in the *Rosa26* locus in mice embryos (Hermann et al. 2012). In accordance with these observations, all *Rosa26* HDR rats analyzed expressed GFP ubiquitously. Thus, integration of other transgenes into the *Hprt1* or *Rosa26* locus via nuclease-stimulated HDR using the donor DNA constructs described in this study should avoid the phenomenon of positional effects and result in transgene expression following the pattern of expression of the promoter used.

This work was done with Sprague-Dawley rats, but other rat strains should also be suitable for HDR-directed genome editing using TALE nucleases, since others have generated knockout rats via NHEJ using TALE nucleases in other strains (Mashimo et al. 2013).

In summary, this report demonstrates the feasibility of TALE nucleases delivered into the zygote to generate rats with targeted, complex, and large transgene insertions. In particular, we targeted transgenes to high-value loci, such as *Rosa26* or *Hprt1*, and replaced DNA sequences in an endogenous locus. This technique is a faster, cheaper, and easier alternative to ES cell manipulation (Dow and Lowe 2012). TALE nucleases now join ZFNs as having effected targeted transgene integration in vivo. CRISPR/Cas9 are even easier to

Table 2. Genotype of all *Hprt1.1-*, *Hprt1.2-*, and *Rosa26*-targeted GFP-positive founders

				Allele KI				
Target	Donor DNA	ID/Sex	No. of alleles	5′ insertion	3′ insertion	Status 2nd allele	RI	Concatemers
Hprt1.1	GFP	37°C-13.1/F	3	+	+	wt, Δ 2 bp	–	+
Hprt1.2	GFP	37°C-1.1/F	2	+	–	wt	–	+
Hprt1.2	GFP	37°C-6.1/F	2	+	+	Δ 110 bp	–	–
Hprt1.2	GFP	37°C-9.6/F	2	+	+	Δ 41 bp	–	+
Hprt1.2	GFP	37°C-11.9/F	2	+	+	Δ 25 bp	–	–
Hprt1.2	GFP	37°C-12.2/M	Mosaic	+	+	Mosaic	–	+
Hprt1.2	GFP	37°C-13.2/F	2	–	–	wt	+	+
Hprt1.2	GFP	30°C-1.2/F	Mosaic	+	+	Mosaic	–	+
Hprt1.2	GFP	30°C-2.2/F	2	+	+	Δ 9 + Ins 1 bp	–	–
Hprt1.2	GFP	30°C-3.2/M	1	–	–	Large Δ	+	+
Hprt1.2	GFP	30°C-3.4/F	2	+	+	Δ 16 bp	–	+
Hprt1.2	GFP	30°C-5.7/F	2	–	–	wt	+	–
Hprt1.2	GFP	30°C-5.9/F	2	+	+	Large Δ	–	–
Hprt1.2	GFP	30°C-6.4/M	1	–	–	Large Δ	+	+
Hprt1.2	GFP	30°C-6.5/F	2	–	–	Δ 16, Δ 22 + Ins 2 bp	+	+
Hprt1.2	GFP	30°C-7.3/F	2	+	+	Large Δ	–	+
Hprt1.2	GFP	30°C-7.5/F	Mosaic	–	–	Mosaic	+	+
Hprt1.2	GFP	30°C-7.8/F	2	–	–	Large Δ	+	–
Hprt1.2	GFP	30°C-8.3/F	2	+	+	Δ 19 bp	–	+
Hprt1.2	GFP	30°C-9.7/F	2	+	+	wt	–	+
Hprt1.2	GFP	30°C-10.2/F	2	+	+	Δ 29 bp	–	+
Hprt1.2	GFP	30°C-10.4/F	2	+	+	Δ 92 bp	–	+
Hprt1.2	GFP	37-30°C-4.4/F	3	+	+	Δ 19, Δ 12 + Ins2 bp	–	+
Hprt1.2	GFP	37-30°C-4.6/F	2	+	+	Δ 15 bp	–	+
Hprt1.2	GFP	37-30°C-5.1/F	2	–	–	Δ 50 bp	+	+
Hprt1.2	GFP	37-30°C-5.3/F	2	+	+	Large Δ	–	+
Hprt1.2	GFP	37-30°C-7.2/M	Mosaic	+	+	Mosaic	–	+
Hprt1.2	GFP	37-30°C-7.4/F	2	+	+	Δ 10 bp	–	–
Hprt1.2	GFP	37-30°C-9.5/F	2	–	–	wt	+	+
Hprt1.2	GFP	37-30°C-10.2/F	3	+	+	wt, Δ 1 bp	–	+
Hprt1.2	GFP	37-30°C-10.7/F	2	+	+	Δ 6 bp	–	+
Hprt1.2	GFP	37-30°C-10.8/M	Mosaic	–	–	Mosaic	+	+
Hprt1.2	GFP	30°C circ-4.1/M	1	–	–	Large Δ	+	–
Rosa26	GFP	37°C-2.1/F	2	+	+	Δ 17 bp	–	–
Rosa26	GFP	37°C-3.1/M	2	+	+	Δ 11 bp	–	+
Rosa26	GFP	37°C-5.3/F	2	–	–	wt, Δ 1 bp	+	nd
Rosa26	GFP	37-30°C-7.1/F	2	–	–	wt	+	–
Rosa26	GFP	37-30°C-8.4/M	Mosaic	+	+	Mosaic	–	–
Rosa26	GFP	37-30°C-8.5/M	2	+	+	Δ 16 bp	–	–
Rosa26	GFP	37-30°C-9.1/F	2	+	+	Large Δ	–	–
Rosa26	GFP	37°C-10.2/F	2	+	+	Large Δ	–	–
Rosa26	GFP	37°C-12.5/M	2	+	+	Δ 8 bp	–	+
Rosa26	GFP	30°C-19.3/F	2	–	–	wt	+	+

ID refers to each day 15 embryo (E15) or live pup carrying an insertion of the transgene by HDR or RI. The culture conditions after microinjection are indicated for each *Hprt1.1-, 1.2-*, and *Rosa26*-positive animals. The *Hprt1* locus is in the X chromosome. Some females with three X alleles or males with two X alleles are explained by mosaicism. As examples, female *Hprt1.1* GFP 37°C-13.1/F had one X chromosome with wild-type sequences, a second one with a KI, and a third one with a 2-bp deletion that originated in NHEJ. Others such as *Hprt1.2 GFP* 37-30°C-4.4/F had one with a KI and two more with NHEJ mutations. Large Δ refers to either fetuses carrying deletions >300 bp in the PCR used to perform the T7 and sequencing analysis–most of these animals did not show amplification using primers amplifying a 700-bp sequence.
(Mosaic) Multiple undefined indels; (nd) not determined; (wt) wild-type allele.

generate and are an important new tool for genome editing, although more work is needed to fully evaluate potential off-target effects.

Methods

Animals

Sprague-Dawley (SD/Crl) rats were the only strain used and were sourced from the Charles River (L'Arbresle, France).

Design and production of TALE nucleases

TALE nucleases were produced as previously described (Piganeau et al. 2013; Auer et al. 2014) by the unit assembly method adapted from Huang et al. (2011) and are described in detail in the Supplemental Material.

In vitro assay of TALE nucleases

Each subunit of TALE nuclease plasmid was nucleofected into C6 cells (Sigma) and DNA analyzed by PCR with specific primers (Supplemental Table S2), followed by the T7 endonuclease I assay (Menoret et al. 2014), as detailed in the Supplemental Material.

In vitro transcription of TALE nucleases mRNA

TALE nuclease plasmids were in vitro transcribed, polyadenylated, purified, and used as described in detail in the Supplemental Material.

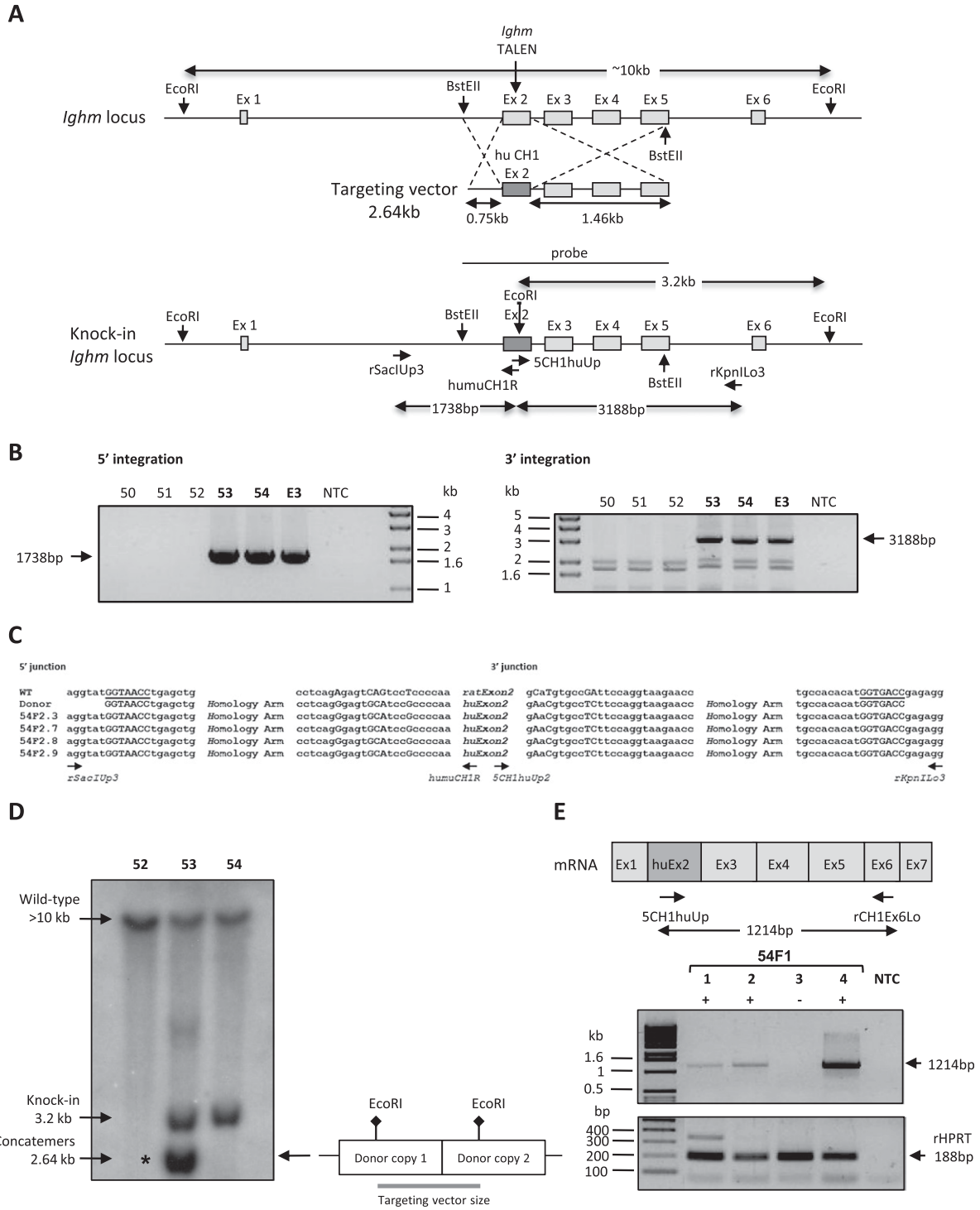

Figure 4. Targeted exon exchange into the rat *Ighm* locus. (*A*) (*Upper*) Diagrams showing schematic representations of the rat *Ighm* locus with the site of TALE nuclease action and of the targeting vector containing exon 2 of human *IGHM* flanked by 0.75-kb-long 5′ and 1.46-kb-long 3′ homology arms. (*Lower*) Diagram showing the integration by homologous recombination of the donor DNA sequence in the targeted locus, and the position of primers used for 5′ and 3′ junction PCRs. Integration in the 5′ and 3′ sides should generate fragments of 1738 bp and 3188 bp, respectively. EcoRI is the restriction enzyme used in Southern blot analyses due to the presence of the EcoRI site in the human but not in the rat *Ighm* sequence. The probe used in Southern blot analyses is the targeting vector. In the case of homologous recombination events, a 3.2-kb band is expected. (*B*) The *left* and *right* gels show the results analyzing, respectively, the 5′ and 3′ extremity of DNA integration, using the pair of primers indicated in *A*. Three animals (53, 54, and E3) showed a band of expected size (1738 bp in 5′ and 3188 bp in 3′ ends). (NTC) No template control. (*C*) Sequence comparison at the 5′ and 3′ junctions with wild-type genomic DNA and donor DNA sequences of four representative F2s (54F2.3, 54F2.7, 54F2. 8, and 54F2.9: F2 generation from animal 54). Exon exchange was confirmed at the BstEII site in 5′ and 3′ (underlined). (*D*) Southern blot analysis of founders for homologous recombination integration. Genomic DNA was digested with EcoRI and 10 µg of DNA were loaded per lane. Blots were probed with the targeting sequence, as indicated in *A*. Arrows indicate bands of 10 kb and 3.2 kb corresponding to wild-type sequences and HDR sequences, respectively. An asterisk marks the presence of concatemers showing a band at 2.64 kb (the size of the transgene). The diagram at the *right* explains the expected size of the concatemers once linearized. Two animals (founders 53 and 54) harbor a HDR insertion, whereas no HDR event is observed in the third (animal 52). More than one copy of the donor DNA sequence is observed in animal 53. (*E*) (*Upper*) Diagrams showing a schematic representation of the mRNA sequence in HDR animals and the position of primers used for RT-PCR. A band of 1214 bp is expected. (*Lower*) Electrophoresis gel pictures show the presence of an amplified band of 1214 bp in three animals born from the mating of the founder 54 (HDR) with a wild-type rat. The amplification of rat HPRT serves as a control. (NTC) No template control.

Table 3. Microinjection statistics for the *Ighm* locus

Donor DNA form	Dose mRNA/DNA (ng/μl)	Temperature	No. injected eggs (% viable eggs)	No. E15 (e) or pups (p) (%)[a]	No. of RI-positive animals (%)[a]	No. of HDR-positive animals (%)[a]	No. of indel-positive animals (%)[a]
Linear[b]	5 + 5/10	37°C	1063 (72.7)	5e – 72p (15.8)	8 (1.64)	3 (0.62)	54 (11.1)
Circular[c]	5 + 5/10	37°C	410 (75.1)	64p (22.9)	2 (0.72)	0 (0)	35 (12.5)

Rat *Ighm* TALE nucleases, as mRNA, were injected at a concentration of 10 ng/μl in combination with 10 ng/μl of donor DNA, either in its linear form or in its circular form, both into the cytoplasm and into the male pronucleus. Injected eggs were maintained under 5% CO_2 at 37°C until reimplantation. Viability was evaluated after the culture period. Potential toxicity was also assessed by the number of day 15 embryos (E15) or of live pups obtained following the transfer of injected eggs. The numbers of E15 or live pups which have integrated the donor DNA sequence either by random integration (RI) or HDR integration (PCR positive both at the 5′ and 3′ ends) or which have indel mutations, are reported in the last three columns.
[a]Percentages indicated in parentheses correspond to the percentage of transferred embryos.
[b]Excised form.
[c]Supercoiled DNA.

Targeting vector construction

Plasmids donor sequences were based on the Brown Norway rat genomic sequence (assembly RGSC_3.4). For the *Hprt1.1*, *Hprt1.2*, and *Rosa26* loci, donor sequences contained a CAG promoter-eGFP cDNA-BGHpA cassette flanked by two 800-bp homologous arms.

For the replacement of rat *Ighm* exon 2, we generated a plasmid containing human *IGHM* exon 2 flanked by rat sequence 5′ and 3′ homology arms (0.75 kb and 1.46 kb, respectively).

The generation and use of these donor DNA sequences is described in detail in the Supplemental Material.

Microinjection of rat one-cell embryos

Fertilized one-cell-stage embryos were sequentially microinjected into the male pronucleus and into the cytoplasm. One-cell embryo collection and manipulation are described in the Supplemental Material.

Analysis of NHEJ events

Briefly, DNA fragments including the TALE nuclease targeted regions were PCR-amplified with a high-fidelity polymerase (Herculase II fusion polymerase) using specific primers (Supplemental Table S2). Mutations were analyzed using the T7 endonuclease I assay (Menoret et al. 2013) and direct sequencing of PCR products.

Analysis of targeted and RI of DNA donor sequences

Donor DNA was amplified using the primer pairs for *GFP*. DNA from GFP+ animals was PCR-amplified with primers situated outside and inside of each extremity of the homology arms as described in detail in the Supplemental Material (Supplemental Table S2). Southern blots were done on genomic DNA digested by EcoRI for *Hprt1.1*, BamHI for *Hprt1.2*, and EcoRI for *Rosa26*.

Analysis of GFP expression

GFP expression was analyzed as described in detail in the Supplemental Material.

Analysis of *Ighm* mRNA

Analysis was performed on total RNA, DNase-treated, and PCR-amplified using primers (Supplemental Table S2) and techniques described in the Supplemental Material section.

Competing interest statement

G.J.C. is a full-time employee of Sangamo BioSciences.

Table 4. Genotypes of all *Ighm*-positive founders analyzed at the target site

Target	Donor DNA	ID/Sex	No. of alleles	Allele KI		Status 2nd allele	RI	Concatemers
				5′ insertion	3′ insertion			
Ighm	huCH1	E3F	2	+	+	Δ 6 bp	–	+
Ighm	huCH1	8/F	Mosaic	–	–	Mosaic	+	nd
Ighm	huCH1	44/F	2	–	–	Δ 84 bp	+	–
Ighm	huCH1	49/M	2	–	–	Δ 27, Δ 6 bp	+	–
Ighm	huCH1	53/M	2	+	+	Δ 5 bp	–	+
Ighm	huCH1	54/M	2	+	+	Δ 12 bp	–	–
Ighm	huCH1	55/F	2	–	–	Δ 16, Δ 16 bp	+	–
Ighm	huCH1	56/F	2	–	–	Δ 1, Δ 1 bp	+	–
Ighm	huCH1	63/F	2	–	–	Δ 5, Δ 5 bp	+	+
Ighm	huCH1	68/M	Mosaic	–	–	Mosaic	+	+
Ighm	huCH1	69/M	2	–	–	nd	+	+
Ighm	huCH1	Circ-81/F	2	–	–	nd	+	nd
Ighm	huCH1	Circ-85/M	2	–	–	wt	+	nd

Circ-81/F and Circ-85/M are the two animals generated with the circular donor DNA whereas all the other animals were generated with the linear excised form. (Mosaic) Multiple undefined indels; (nd) not determined.

Acknowledgments

Funding was provided by Région Pays de la Loire through Biogenouest, IBiSA program, Fondation Progreffe and TEFOR (Infrastructures d'Avenir of the French government). Sequencing experiments were performed by the integrative genomic facility of Nantes and Gregory J. Cost from Sangamo.

Author contributions: I.A., A.F., L.T., S.R., and S.M. conceived and designed the experiments. M.C., J.B.R., A.D.C., J.P.C., and C.G. performed the design, production, and in vitro assay of *Hprt1* and *Rosa26* TALE nucleases. G.J.C. designed and produced *Ighm* TALE nucleases and edited the manuscript. R.B. generated the *IGHM* DNA construct. L.T. performed in vitro transcription of TALE nucleases, built donor constructs, and carried out PCR and Southern blot analyses. V.T., R.T., and L.T. performed the T7 assay. S.R., S.M., and C.U. performed the microinjections. D.B. performed the statistical analyses. S.R. performed the FACS experiments and microscopy. S.R., L.T., and I.A. wrote the manuscript.

References

Auer TO, Duroure K, De Cian A, Concordet JP, Del Bene F. 2014. Highly efficient CRISPR/Cas9-mediated knock-in in zebrafish by homology-independent DNA repair. *Genome Res* **24:** 142–153.

Beumer KJ, Trautman JK, Bozas A, Liu JL, Rutter J, Gall JG, Carroll D. 2008. Efficient gene targeting in *Drosophila* by direct embryo injection with zinc-finger nucleases. *Proc Natl Acad Sci* **105:** 19821–19826.

Brinster RL, Chen HY, Trumbauer ME, Yagle MK, Palmiter RD. 1985. Factors affecting the efficiency of introducing foreign DNA into mice by microinjecting eggs. *Proc Natl Acad Sci* **82:** 4438–4442.

Brinster RL, Braun RE, Lo D, Avarbock MR, Oram F, Palmiter RD. 1989. Targeted correction of a major histocompatibility class II E α gene by DNA microinjected into mouse eggs. *Proc Natl Acad Sci* **86:** 7087–7091.

Bronson SK, Plaehn EG, Kluckman KD, Hagaman JR, Maeda N, Smithies O. 1996. Single-copy transgenic mice with chosen-site integration. *Proc Natl Acad Sci* **93:** 9067–9072.

Brown AJ, Fisher DA, Kouranova E, McCoy A, Forbes K, Wu Y, Henry R, Ji D, Chambers A, Warren J, et al. 2013. Whole-rat conditional gene knockout via genome editing. *Nat Methods* **10:** 638–640.

Buehr M, Meek S, Blair K, Yang J, Ure J, Silva J, McLay R, Hall J, Ying QL, Smith A. 2008. Capture of authentic embryonic stem cells from rat blastocysts. *Cell* **135:** 1287–1298.

Capecchi MR. 2005. Gene targeting in mice: functional analysis of the mammalian genome for the twenty-first century. *Nat Rev Genet* **6:** 507–512.

Chen CM, Krohn J, Bhattacharya S, Davies B. 2011. A comparison of exogenous promoter activity at the *ROSA26* locus using a PhiC31 integrase mediated cassette exchange approach in mouse ES cells. *PLoS ONE* **6:** e23376.

Cristea S, Freyvert Y, Santiago Y, Holmes MC, Urnov FD, Gregory PD, Cost GJ. 2013. In vivo cleavage of transgene donors promotes nuclease-mediated targeted integration. *Biotechnol Bioeng* **110:** 871–880.

Cui X, Ji D, Fisher DA, Wu Y, Briner DM, Weinstein EJ. 2011. Targeted integration in rat and mouse embryos with zinc-finger nucleases. *Nat Biotechnol* **29:** 64–67.

Dai J, Cui X, Zhu Z, Hu W. 2010. Non-homologous end joining plays a key role in transgene concatemer formation in transgenic zebrafish embryos. *Int J Biol Sci* **6:** 756–768.

Dow LE, Lowe SW. 2012. Life in the fast lane: mammalian disease models in the genomics era. *Cell* **148:** 1099–1109.

Doyon Y, Choi VM, Xia DF, Vo TD, Gregory PD, Holmes MC. 2010. Transient cold shock enhances zinc-finger nuclease-mediated gene disruption. *Nat Methods* **7:** 459–460.

Flisikowska T, Thorey IS, Offner S, Ros F, Lifke V, Zeitler B, Rottmann O, Vincent A, Zhang L, Jenkins S, et al. 2011. Efficient immunoglobulin gene disruption and targeted replacement in rabbit using zinc finger nucleases. *PLoS ONE* **6:** e21045.

Gao Q, Reynolds GE, Innes L, Pedram M, Jones E, Junabi M, Gao DW, Ricoul M, Sabatier L, Van Brocklin H, et al. 2007. Telomeric transgenes are silenced in adult mouse tissues and embryo fibroblasts but are expressed in embryonic stem cells. *Stem Cells* **25:** 3085–3092.

Garrick D, Fiering S, Martin DI, Whitelaw E. 1998. Repeat-induced gene silencing in mammals. *Nat Genet* **18:** 56–59.

Geurts AM, Cost GJ, Freyvert Y, Zeitler B, Miller JC, Choi VM, Jenkins SS, Wood A, Cui X, Meng X, et al. 2009. Knockout rats via embryo microinjection of zinc-finger nucleases. *Science* **325:** 433.

Hermann M, Maeder ML, Rector K, Ruiz J, Becher B, Burki K, Khayter C, Aguzzi A, Joung JK, Buch T, et al. 2012. Evaluation of OPEN zinc finger nucleases for direct gene targeting of the *ROSA26* locus in mouse embryos. *PLoS ONE* **7:** e41796.

Huang P, Xiao A, Zhou M, Zhu Z, Lin S, Zhang B. 2011. Heritable gene targeting in zebrafish using customized TALENs. *Nat Biotechnol* **29:** 699–700.

Jacob HJ. 1999. Functional genomics and rat models. *Genome Res* **9:** 1013–1016.

Jacob HJ. 2010. The rat: a model used in biomedical research. *Methods Mol Biol* **597:** 1–11.

Jacob HJ, Kwitek AE. 2002. Rat genetics: attaching physiology and pharmacology to the genome. *Nat Rev Genet* **3:** 33–42.

Johnson RD, Jasin M. 2001. Double-strand-break-induced homologous recombination in mammalian cells. *Biochem Soc Trans* **29:** 196–201.

Katsuyama T, Akmammedov A, Seimiya M, Hess SC, Sievers C, Paro R. 2013. An efficient strategy for TALEN-mediated genome engineering in *Drosophila*. *Nucleic Acids Res* **41:** e163.

Kobayashi T, Kato-Itoh M, Yamaguchi T, Tamura C, Sanbo M, Hirabayashi M, Nakauchi H. 2012. Identification of rat *Rosa26* locus enables generation of knock-in rat lines ubiquitously expressing *tdTomato*. *Stem Cells Dev* **21:** 2981–2986.

Li P, Tong C, Mehrian-Shai R, Jia L, Wu N, Yan Y, Maxson RE, Schulze EN, Song H, Hsieh CL, et al. 2008. Germline competent embryonic stem cells derived from rat blastocysts. *Cell* **135:** 1299–1310.

Li D, Qiu Z, Shao Y, Chen Y, Guan Y, Liu M, Li Y, Gao N, Wang L, Lu X, et al. 2013a. Heritable gene targeting in the mouse and rat using a CRISPR-Cas system. *Nat Biotechnol* **31:** 681–683.

Li W, Teng F, Li T, Zhou Q. 2013b. Simultaneous generation and germline transmission of multiple gene mutations in rat using CRISPR-Cas systems. *Nat Biotechnol* **31:** 684–686.

Maresca M, Lin VG, Guo N, Yang Y. 2013. Obligate ligation-gated recombination (ObLiGaRe): custom-designed nuclease-mediated targeted integration through nonhomologous end joining. *Genome Res* **23:** 539–546.

Mashimo T, Takizawa A, Voigt B, Yoshimi K, Hiai H, Kuramoto T, Serikawa T. 2010. Generation of knockout rats with X-linked severe combined immunodeficiency (X-SCID) using zinc-finger nucleases. *PLoS ONE* **5:** e8870.

Mashimo T, Kaneko T, Sakuma T, Kobayashi J, Kunihiro Y, Voigt B, Yamamoto T, Serikawa T. 2013. Efficient gene targeting by TAL effector nucleases coinjected with exonucleases in zygotes. *Sci Rep* **3:** 1253.

Meek S, Buehr M, Sutherland L, Thomson A, Mullins JJ, Smith AJ, Burdon T. 2010. Efficient gene targeting by homologous recombination in rat embryonic stem cells. *PLoS ONE* **5:** e14225.

Menoret S, Fontaniere S, Jantz D, Tesson L, Thinard R, Remy S, Usal C, Ouisse LH, Fraichard A, Anegon I. 2013. Generation of *Rag1*-knockout immunodeficient rats and mice using engineered meganucleases. *FASEB J* **27:** 703–711.

Menoret S, Tesson L, Remy S, Usal C, Thepenier V, Thinard R, Ouisse LH, De Cian A, Giovannangeli C, Concordet JP, et al. 2014. Gene targeting in rats using transcription activator-like effector nucleases. *Methods* doi: 10.1016/j.ymeth.2014.02.027.

Meyer M, de Angelis MH, Wurst W, Kuhn R. 2010. Gene targeting by homologous recombination in mouse zygotes mediated by zinc-finger nucleases. *Proc Natl Acad Sci* **107:** 15022–15026.

Meyer M, Ortiz O, Hrabe de Angelis M, Wurst W, Kuhn R. 2012. Modeling disease mutations by gene targeting in one-cell mouse embryos. *Proc Natl Acad Sci* **109:** 9354–9359.

Miller JC, Tan S, Qiao G, Barlow KA, Wang J, Xia DF, Meng X, Paschon DE, Leung E, Hinkley SJ, et al. 2011. A TALE nuclease architecture for efficient genome editing. *Nat Biotechnol* **29:** 143–148.

Milot E, Strouboulis J, Trimborn T, Wijgerde M, de Boer E, Langeveld A, Tan-Un K, Vergeer W, Yannoutsos N, Grosveld F, et al. 1996. Heterochromatin effects on the frequency and duration of LCR-mediated gene transcription. *Cell* **87:** 105–114.

Ochiai H, Sakamoto N, Fujita K, Nishikawa M, Suzuki K, Matsuura S, Miyamoto T, Sakuma T, Shibata T, Yamamoto T. 2012. Zinc-finger nuclease-mediated targeted insertion of reporter genes for quantitative imaging of gene expression in sea urchin embryos. *Proc Natl Acad Sci* **109:** 10915–10920.

Panda SK, Wefers B, Ortiz O, Floss T, Schmid B, Haass C, Wurst W, Kuhn R. 2013. Highly efficient targeted mutagenesis in mice using TALENs. *Genetics* **195:** 703–713.

Pedram M, Sprung CN, Gao Q, Lo AW, Reynolds GE, Murnane JP. 2006. Telomere position effect and silencing of transgenes near telomeres in the mouse. *Mol Cell Biol* **26:** 1865–1878.

Piganeau M, Ghezraoui H, De Cian A, Guittat L, Tomishima M, Perrouault L, Rene O, Katibah GE, Zhang L, Holmes MC, et al. 2013. Cancer translocations in human cells induced by zinc finger and TALE nucleases. *Genome Res* **23:** 1182–1193.

Ponce de Leon V, Merillat AM, Tesson L, Anegon I, Hummler E. 2014. Generation of TALEN-mediated GR^{dim} knock-in rats by homologous recombination. *PLoS ONE* **9:** e88146.
Segal DJ, Meckler JF. 2013. Genome engineering at the dawn of the golden age. *Annu Rev Genomics Hum Genet* **14:** 135–158.
Sommer D, Peters A, Wirtz T, Mai M, Ackermann J, Thabet Y, Schmidt J, Weighardt H, Wunderlich FT, Degen J, et al. 2014. Efficient genome engineering by targeted homologous recombination in mouse embryos using transcription activator-like effector nucleases. *Nat Commun* **5:** 3045.
Tesson L, Cozzi J, Menoret S, Remy S, Usal C, Fraichard A, Anegon I. 2005. Transgenic modifications of the rat genome. *Transgenic Res* **14:** 531–546.
Tesson L, Usal C, Menoret S, Leung E, Niles BJ, Remy S, Santiago Y, Vincent AI, Meng X, Zhang L, et al. 2011. Knockout rats generated by embryo microinjection of TALENs. *Nat Biotechnol* **29:** 695–696.
Tong C, Li P, Wu NL, Yan Y, Ying QL. 2010. Production of p53 gene knockout rats by homologous recombination in embryonic stem cells. *Nature* **467:** 211–213.
Tong C, Huang G, Ashton C, Wu H, Yan H, Ying QL. 2012. Rapid and cost-effective gene targeting in rat embryonic stem cells by TALENs. *J Genet Genomics* **39:** 275–280.
Wang H, Hu YC, Markoulaki S, Welstead GG, Cheng AW, Shivalila CS, Pyntikova T, Dadon DB, Voytas DF, Bogdanove AJ, et al. 2013. TALEN-mediated editing of the mouse Y chromosome. *Nat Biotechnol* **31:** 530–532.
Wefers B, Meyer M, Ortiz O, Hrabe de Angelis M, Hansen J, Wurst W, Kuhn R. 2013. Direct production of mouse disease models by embryo microinjection of TALENs and oligodeoxynucleotides. *Proc Natl Acad Sci* **110:** 3782–3787.
Williams A, Harker N, Ktistaki E, Veiga-Fernandes H, Roderick K, Tolaini M, Norton T, Williams K, Kioussis D. 2008. Position effect variegation and imprinting of transgenes in lymphocytes. *Nucleic Acids Res* **36:** 2320–2329.
Yamamoto S, Nakata M, Sasada R, Ooshima Y, Yano T, Shinozawa T, Tsukimi Y, Takeyama M, Matsumoto Y, Hashimoto T. 2012. Derivation of rat embryonic stem cells and generation of protease-activated receptor-2 knockout rats. *Transgenic Res* **21:** 743–755.
Zambrowicz BP, Imamoto A, Fiering S, Herzenberg LA, Kerr WG, Soriano P. 1997. Disruption of overlapping transcripts in the ROSA βgeo 26 gene trap strain leads to widespread expression of β-galactosidase in mouse embryos and hematopoietic cells. *Proc Natl Acad Sci* **94:** 3789–3794.
Zheng S, Geghman K, Shenoy S, Li C. 2012. Retake the center stage–new development of rat genetics. *J Genet Genomics* **39:** 261–268.

Received December 20, 2013; accepted in revised form April 16, 2014.